UDC 541.128-022.532

CATALYSTS FOR ANODE OXIDATION OF FORMIC ACID ON CARBON NANOTUBES "TAUNIT"*

N.A. Yashtulov@, M.V. Lebedeva, S.M. Pestov

Moscow Technological University (Institute of Fine Chemical Technologies), Moscow, 119571 Russia
**Corresponding author e-mail: YashtulovNA@mail.ru*

Platinum-palladium/carbon nanotubes (CNT) carbon nanocomposites were synthesized by chemical reduction of ions in water-organic solutions of reverse microemulsions. Physico-chemical characteristics of the nanocomposites were studied by atomic force microscopy, transmission electron microscopy, photon-correlation spectroscopy, X-ray phase analysis and chronopotentiometry. It was found that the smallest platinum-palladium nanoparticles size is observed when the metal ratio is 3:1 and the water pool size is minimal (ω = 1.5). Testing of catalytic activity in the oxidation of formic acid showed that the platinum-palladium/CNT nanocomposites showed higher corrosion resistance than nanocomposites with pure palladium.

Keywords: *nanocatalysts, carbon nanotubes, electron microscopy, chronopotentiometry.*

Introduction

By now certain success has been achieved in the field of nanomaterials chemistry and technology. Thanks to the wide potentialities of using nanomaterials in such fields of science and technology as power economy, electronics, electrochemistry, catalysis etc. their studies have been intensively developed [1−5]. In particular, an important stage of the studies development is associated with systematic studying of processes that proceed when obtaining nanoelectrocatalysts on interphase boundaries. This has allowed suggesting techniques for the formation of nanostructured materials with optimal technological parameters for chemical energy converters [1, 3−12].

In Russian and foreign works much attention is paid to the creation of power sources using direct oxidation of formic acid [8, 9, 12−14]. Developing efficient anode electrocatalysts with high catalytic activity and resistance to the poisoning effect of carbon monoxide is a major problem in the commercialization of fuel cells with direct oxidation of formic acid [1−7]. Numerous studies of HCOOH anode oxidation catalysts based on platinum and palladium [4, 7, 9−12] are being performed. Formic acid oxidation on platinum catalysts occurs predominantly with the formation of carbon monoxide as an intermediate product, the molecules of which block active sites of the platinum catalyst [7, 9]. It is shown [4, 9, 10, 12] that when using low-temperature fuel cells, palladium nanoparticles have higher catalytic activity in formic acid anode oxidation as compared to similar platinum catalysts. The reason is that the oxidation reaction proceeds via the "direct" path without CO formation. However,

* Original Russian Text © N.A. Yashtulov, M.V. Lebedeva, S.M. Pestov, 2016, published in Tonkie Khimicheskie Tekhnologii / Fine Chemical Technologies, 2016, Vol. 11, No 5, pp. 51-56.

the main disadvantage of palladium catalysts as opposed to platinum ones is lower corrosion resistance in acidic environments [7]. Therefore, using platinum and palladium in combined bi- and polymetallic catalysts of HCOOH oxidation [8, 9, 13, 14] is promising. It was found that adding palladium nanoparticles to a platinum catalyst on carbon a carrier (soot, KhS-72) decreases the activation energy of HCOOH oxidation, and the reaction proceeds mostly via the direct path without noticeable formation of CO molecules [9].

Tasks aimed to the increase in current sources efficiency can be solved by applying carrier matrixes made of carbon with high specific surface, nanostructured solid polymer membranes modified by nanoparticles of electrocatalysts. Using nanofibres and nanotubes as catalyst carriers allows not only considerably improving specific characteristics of current sources, but also reducing catalyst consumption and increasing its operating life [1, 2, 4, 8, 9, 12−14].

In this work platinum-palladium nanoparticles were obtained in water-organic solutions of reversed micelles by the chemical reduction of metal ions with the use of an anionic surface-active substance – sodium bis(2-ethylhexyl)sulphosuccinate (AOT). The synthesized metal nanoparticles were precipitated on the surface of Taunit carbon nanotubes (CNT) for the formation of platinum-palladium/CNT nanocomposites. Such hybrid nanostructures have high catalytic activity and stability [8, 9, 12−14].

The work purpose was to synthesize bimetallic platinum-palladium nanocatalysts on Taunit carbon nanotubes and estimate the nanocatalysts catalytic activity in the anodic oxidation of formic acid.

Experimental

Solutions of bimetallic platinum-palladium nanoparticles were obtained by the chemical reduction of metal ions in reversed microemulsions, which was previously described in detail [10, 11, 15]. Reversed microemulsions are microscopic drops of an aqueous solution of a salt – pools stabilized by a surfactant in an organic solvent (hexane). The water/surfactant molar ratio (ω) in the experiments varied from 1.5 to 8. Aqueous solutions of platinum metal salts $H_2[PtCl_6]$ and $[Pd(NH_3)_2Cl_2]$ ("Sigma Aldrich", USA) at concentration 0.02 M served as precursors for the synthesis of bimetallic nanoparticles. Pt:Pd molar ratio was 1:1, 1:3 and 1:5. In order to form bimetallic nanoparticles two solutions were prepared. The first one was a solution of precursors with an addition of a 0.15 M AOT solution (99%, "Sigma Aldrich",

USA) in isooctane. The second solution contained a surfactant solution with a reducer – 0.12 M aqueous solution of sodium tetrahydroborate $NaBH_4$ ("Merck", Germany) [10, 11]. Carbon ink was obtained by dissolving 0.1 g of carbon nanotubes in 3 ml of bidistilled water. The synthesis of platinum-palladium/CNT nanocomposites of controlled structure was carried out by mixing aqueous-organic solutions of metal salts (the first solution) with a solution of carbon ink followed by stirring for 30 min. Then a solution of the reducer (the second solution) was added under stirring to the obtained solution. Solubilization of the solutions was carried out in an ultrasonic dispergator Ultrasonis Cleaner UD150SH-6L ("Eumax", Germany) for 1–2 min at 25±1°C. In order to form nanocatalysts Taunit carbon nanotubes were used (a certified domestic product, the Russian Federation, Tambov).

The sizes, form and distribution of platinum-palladium nanoparticles were investigated by atomic force microscopy (AFM) on an NTegra Prima scanning microscope ("NT MDT", Russia). The morphology of polymer films surface was studied by high-resolution transmission electron microscopy (HRTEM) on a Zeiss Libra 200FE device ("Carl Zeiss", Germany). The sizes of water pool aggregates in the solutions of the reversed microemulsions were determined by dynamic laser light scattering on a Delsa Nano particle analyzer ("Beckman Coulter", Ireland). The phase structure of bimetallic nanocomposites was studied on a D8 FOCUS powder X-ray diffractometer ("Bruker AXS", Germany) with filtered CuK_α radiation in a step mode, with an acquisition time of 5 s and a step width of 0.5°). Chronopotentiometric measurements were carried out on an IPC PRO M device (Tekhnopribor, Russia).

Results and Discussion

In order to determine the optimal conditions for synthesizing nanocomposites, the influence of the precursors' characteristics on nanoparticle sizes in aqueous-organic solutions was estimated. The study of nanoparticle sizes and shapes was carried out in the semi-contact mode by means of atomic force microscopy (AFM). Reversed micellar solutions of platinum-palladium nanoparticles were analyzed on a standard substrate of mica.

Fig. 1 shows an image of Pt-Pd nanoparticles obtained by AFM at the metals ratio 3:1 and solubilization coefficient $\omega = 1.5$. The preferential formation of ellipse nanoparticles with sizes 4−5.5 nm is typical of Pt-Pd nanoparticles. Table 1 shows data on the sizes of Pt-Pd nanoparticles in aqueous-organic solutions of reversed microemulsions depending on the metals ratio and solubilization coefficient ω.

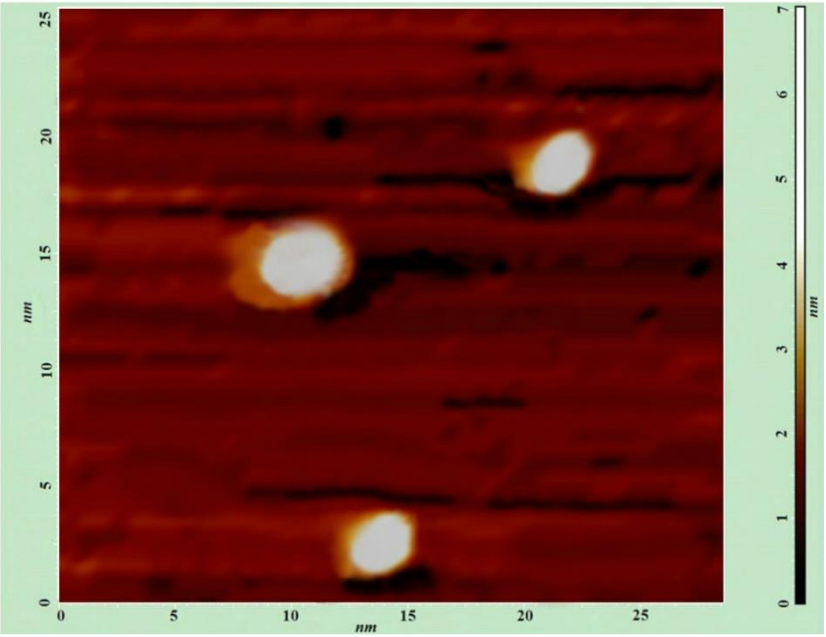

Figure 1. AFM image of Pt-Pd (3:1) nanoparticles at ω = 1.5.

Table 1. Pt-Pd nanoparticle sizes at different content of the metals and solubilization degree ω

Pt : Pd ratio	d, nm			
	ω = 1.5	ω = 3	ω = 5	ω = 8
3 : 1	3.9−5.1	5.3−6.7	6.5−7.4	7.2−8.9
1 : 1	5.6−6.9	6.4−7.6	7.2−8.3	8.7−10.9
1 : 3	6.2−7.5	7.1−8.5	8.1−9.6	12.1−13.4

The results of studying the bimetallic Pt-Pd nanoparticles by atomic force microscopy showed that:

1) The smallest nanoparticles size is typical of nanoparticles with the metals ratio 3:1 and the minimum water pool size ω = 1.5.
2) When the metals ratio is 1:1 and 1:3, and solubilization degree ω is increased to 8, the nanoparticles size increases.

The analysis of the data obtained by atomic force microscopy is complemented by the results of photon-correlation spectroscopy (PCS). The intensity of scattered light (I) measured by this method is determined in dynamic conditions by the rate of particles diffusion (D) in the liquid. This value is inversely proportional to their hydrodynamic diameter corresponding to the sizes of the reversed micelles and micellar complexes. Literature data [16, 17] show the

unique dependence of water pool diameter and the size of a separate microemulsion on the extent of solubilization. In case of AOT/isooctane system theoretical calculation of micelle size gives values from 1.8 to 2.5 nm for the extent of solubilization from 1.5 to 5. Experiments [17] on the isolation of silver nanoparticles fractions in reversed micelles with the use of size-exclusion HPLC showed that PCS provides the sizes of micelle aggregates. Table 2 shows the results of distribution of water pools of micelles with Pt-Pd (3:1) nanoparticles by the sizes (d) and scattering intensity (I) depending on solubilization coefficient ω. It can be concluded on the basis of PCS data that there are three main fractions of water pools of micelles with bimetallic Pt-Pd nanoparticles.

Table 2. Distribution of water pools of micelles with Pt-Pd (3:1) nanoparticles by the sizes (d) and scattering intensity (I) depending on solubilization coefficient ω according to PCS

Fraction	ω = 1.5		ω = 3		ω = 5	
	d, nm	I, %	d, nm	I, %	d, nm	I, %
1	25−38	75	29−44	60	36−51	50
2	41−52	15	47−58	25	56−69	30
3	61−76	10	65−81	15	77−88	20

When the initial concentration of the platinum metals in the water pools of micelles is identical, the metals ratio in the fractions is determined by the pool sizes proportional to solubilization degree ω and by the share of this fraction in aqueous-organic solutions [10, 11, 16]. The PCS results indicate that aggregation of water pools of micelles with sizes from 25 to 88 nm in the organic phase occurs in the course of the nanoparticles synthesis. It can be seen from Table 2 that the sizes of the aggregates increase with increasing water/surfactant molar ratio. This is probably due to stronger intermicellar interaction upon increasing the sizes of water pools. Note that the contribution of small particles increases with growing sizes of the water pools of micelles at the same solubilization degree.

In order to prevent the formation of large nanoparticles of the platinum metals when forming nanocomposites on carbon nanotubes, ultrasound processing of samples was applied. The efficiency of using ultrasound impact is confirmed by AFM (Figure 1) and HRTEM (Figure 2).

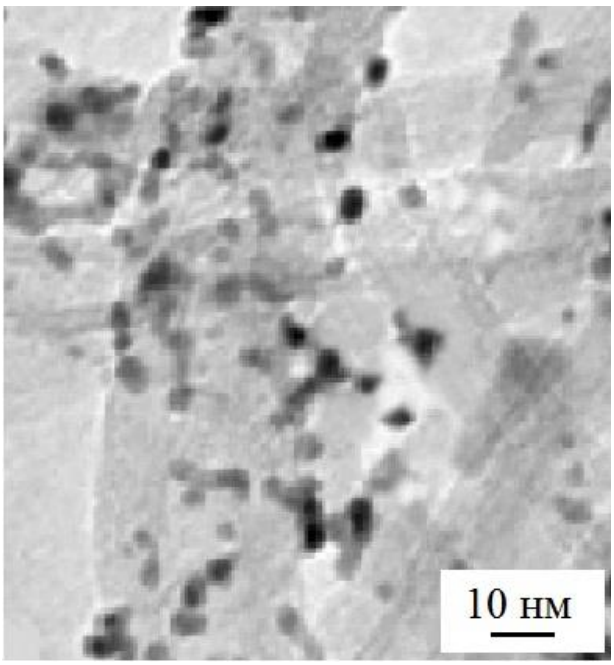

Figure 2. HRTEM images of Pt-Pd (3:1) nanoparticles on carbon nanotubes.

Figure 2 shows an exemplary image of Pt-Pd (3:1) nanoparticles on CNT obtained by high-resolution transmission electron microscopy. Obviously, Pt-Pd nanoparticles are evenly distributed on the CNT surface, and the average particle size is 4−6 nm.

Figure 3 shows X-ray powder diffraction data for Pd/CNT, Pt-Pd (3:1)/CNT and Pt/CNT catalysts. The broadening of the reflexes is probably due to the formation of small particles [5]. It should be emphasized that no additional diffraction peaks that could be attributed to the formation of Pt-Pd oxides are observed on the diffractograms. The pronounced diffraction peaks at 26.5° and 42.8° are attributed to the hexagonal structure of graphite (002) and (100). Therefore, the CNTs have the crystal lattice of graphite and are characterized by high electrical conductance. The diffraction peaks at 2θ = 40.1°, 48.2°, 67.9° and 81.2° are attributed to Pt-Pd (111), (200), (220) and (311) reflexes, respectively, and the diffraction peaks of the nanocomposites based on Pt-Pd practically coincide with the peaks of monometallic Pt and Pd nanocomposites.

In order to calculate the average size of the metal particles according to the Debye-Scherrer equation we chose the Pt-Pd (220) peak [18]. Values 2, 4.6 and 5.4 nm were obtained for Pt/CNT, Pt-Pd/CNT and Pd/CNT, respectively. When using the method of reduction with AOT surfactant, the average particle size increases with increasing Pd content in the catalyst. At the same time the diffraction peaks slightly move towards larger angles, which indicates a small change in the crystal lattice parameters.

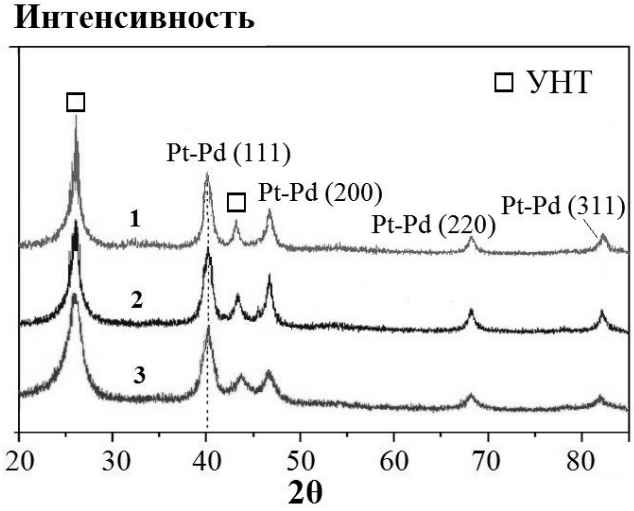

Figure 3. Diffractogram of catalysts on carbon nanotubes:
1) Pt-Pd (3:1)/CNT; 2) Pd/CNT; 3) Pt/CNT.
[Интенсивность means Intensity; УНТ means CNT]

A specific feature of the method for modifying Taunit carbon nanotubes with platinum-palladium nanoparticles suggested in this work consists in activation of the carbon matrix surface with molecular hydrogen in the course of simultaneous reduction of metal ions with sodium tetrahydroborate and sorption of the formed nanoparticles on the CNT. Processing the nanotubes surface with hydrogen promotes the formation of platinum palladium/CNT nanocomposites due to reduction of the oxide-hydroxide forms of carbon typical of Taunit-type CNTs.

An essential indicator of nanocatalysts performance in fuel cells is their stabilization on the matrix substrate preventing agglomeration of catalyst particles as a part of membrane-electrode blocks. The synthesized samples on carbon nanotubes (Pt-Pd (3:1)/CNT and Pd/CNT), as well as the corresponding samples on soot Vulkan KhS-72 (Pt-Pd (3:1)/KhS and Pd/KhS) were tested for catalytic activity in the course of amperochronometric analysis of current density change in time at a fixed potential of formic acid oxidation, E = 0.3 V (Figure 4). It was found that the Pt-Pd (3:1)/CNT nanocatalysts show much higher stability than the Pd/CNT sample without platinum. Current density (j) decreases in the course of 4 h testing by 7% in case of the Pt-Pd/CNT sample and by 16% in case of the Pd/CNT sample. Pt-Pd/CNT (3:1) nanocomposites are characterized by higher corrosion resistance than nanocomposites with pure palladium. In case of commercial Pt-Pd catalysts on KhS-72 soot [9] current density in the course of 4 h testing is 20–25% less as compared to the Pt-Pd/CNT nanocomposites obtained in this work. The presented results confirm the possibility of forming stable high-efficiency palladium-platinum nanocatalysts on Taunit carbon nanotubes for formic acid oxidation.

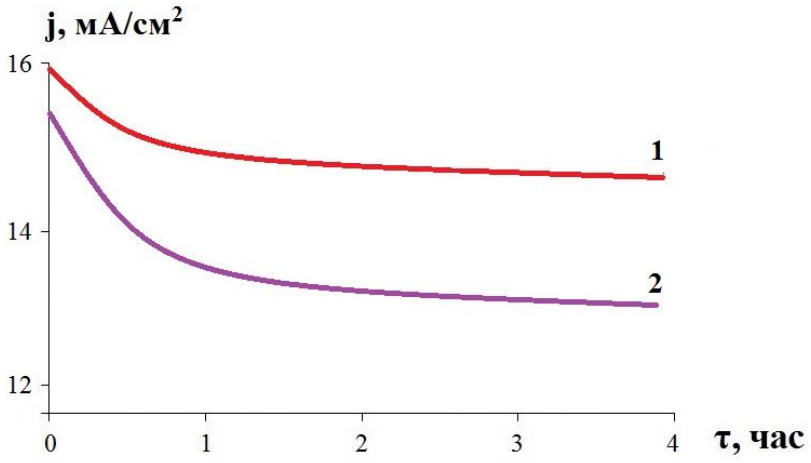

Figure 4. Change in the catalytic activity of Pt-Pd (3:1)/CNT (1) and Pd/CNT (2) nanocatalysts in the reaction of HCOOH oxidation.

[мА/см^2 means mA/cm^2; час means h]

Conclusions

Bimetallic Pt-Pd nanoparticles on Taunit carbon nanotubes were obtained for the first time by the chemical reduction of metal ions in reversed microemulsions with the use of anionic surfactant AOT and studied. These composites can be used as promising catalysts of formic acid oxidation in chemical energy converters.

Acknowledgment

The work was performed with the financial support of the Russian Foundation for Basic Research (project No. 13-08-12407- офи_м2).

References:

1. Stolten D., Emonts B. Fuel Cell Science and Engineering: Materials, Processes, Systems and Technology. Wiley-VCH Verlag GmbH & Co KGaA, 2012. V. 1-2. 1268 p.
2. Gandia L.M., Arzamedi G. Renewable Hydrogen Technologies: Production, Purification, Storage, Applications and Safety. Elsevier, 2013. 472 p.
3. Ghenciu A.F. // Current Opinion in Solid State and Materials Science. 2002. V. 6. № 5. P. 389–399.
4. Rabis A., Paramaconi R., Schmidt T.J. // ACS Catal. 2012. V. 2. № 5. P. 864–890.
5. Tiwari J.N., Tiwari R.N., Singh G., Kim K.S. // Nano Energy. 2013. V. 2. P. 553–578.
6. Tarasevich M.R., Kuzov A.V. // Alternative Energy and Ecology. 2010. V. 87. № 7. P. 86–108.
7. Waszczuk P., Barnard T., Rice C., Masel R., Wieckowscki A. // Electrochem. Commun. 2002. V. 4. № 7. P. 599–603.
8. Winjobi O., Zhang Z., Liang C., Li W. // Electrochim. Acta. 2010. V. 55. № 13. P. 4217–4221.
9. Hong P., Luo F., Liao S., Zeng J. // Int. J. Hydr. Energy. 2011. V. 36. № 14. P. 8518–8524.
10. Yashtulov N.A., Flid V.R. // Russian Chemical Bulletin. 2013. Vol. 62. № 6. P. 1332–1337. (in Russ.)
11. Lebedeva M.V., Yashtulov N.A., Minina N.E., Belyaev B.A. // Vestnik MITHT (Fine Chem. Tech.) 2014. V. 9. № 3. P. 74–78. (in Russ.)
12. Wang J., Yin G., Chen Y., Li R., Sun X. // Int. J. Hydrogen Energy. 2009. V. 34. № 19. P. 8270–8275.
13. Liu B., Li H.Y., Die L., Zhang X.H., Fan Z., Chen J.H. // J. Power Sources. 2009. V. 186. № 1. P. 62–66.
14. Zhang H.X., Wang C., Wang J.Y., Zhai J.J., Cai W.B. // J. Phys Chem C. 2010. V. 114. № 14. P. 6446–6451.
15. Yashtulov N.A., Zenchenko V.O., Lebedeva M.V., Samojlov V.M., Karimov O.Kh., Flid V.R. // Russian Chemical Bulletin. 2016. V. 65. № 1. P. 133–138. (in Russ.)
16. Nevidimov A.V., Razumov V.F. // Molecular Physics. 2009. V. 107. № 20. P. 2169–2180. (in Russ.)
17. Egorova E.M., Revina A.A. // Colloid Journal. 2002. V. 64. № 3. P. 334–345. (in Russ.)
18. Tcybulya S.V., Cherepanova S.V. Vvedenie v strukturnyj analiz nanokristallov (Introduction to the structural analysis of nanocrystals). Novosibirsk: NGU, 2008. 92 p. (in Russ.)